ORGANOMETALLICS

Communication

Cite This: *Organometallics* XXXX, XXX, XXX−XXX

Electrolyte-Free Dye-Sensitized Solar Cell with High Open Circuit Voltage Using a Bifunctional Ferrocene-Based Cyanovinyl Molecule as Dye and Redox Couple

A. Ghosh,[†] S. Mishra,[†] S. Giri,[‡] S. M. Mobin,[§] A. Bera,[*,‖] and S. Chatterjee[*,†]

[†]Department of Chemistry, National Institute of Technology Rourkela, Rourkela, Orissa 769008, India

[‡]Theoretical Chemistry Laboratory, Department of Chemistry, National Institute of Technology Rourkela, Rourkela, Orissa 769008, India

[§]Discipline of Chemistry, Indian Institute of Technology Indore, Simrol, Madhya Pradesh 452017, India

[‖]Department of Physics, Indian Institute of Technology Jammu, Jammu, Jammu and Kashmir 181121, India

Supporting Information

ABSTRACT: Functionalization of ferrocenyl moieties with a cyanovinyl system using a unique solid-state synthetic method led to the formation of donor−acceptor type compounds with wide absorption in the visible region. A DSSC study using the ferrocenyl cyanovinyl compound as a dye with an electrolyte-free fabrication system showed an unprecedented open-circuit voltage (V_{OC}) of 763−841 mV. DFT calculations were carried out to understand an unique electron transfer mechanism for the DSSC device which may be responsible for the high V_{OC}.

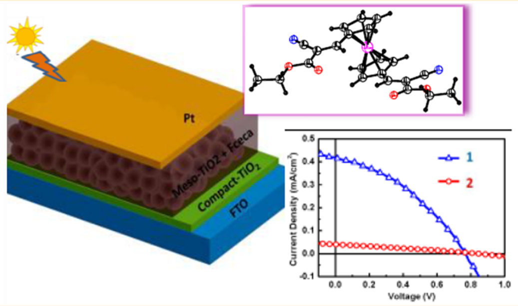

Integrating additional functionalities to a functional material and applying them in useful devices are universal strategies to design multifunctional materials. Ferrocene-based organometallic compounds have gained a great deal of research attention because of their interesting properties related to redox switching, optical nonlinearity, electronic communication, molecular receptor, sensors, etc.[1−6] Recently, substantial interest has been given to ferrocenyl molecules containing a donor−acceptor system because of their unique photophysical and optical properties.[7−10] The intrinsic redox property of the ferrocenyl fragment has made it a potential candidate in dye-sensitized solar cells (DSSC), mostly as a redox electrolyte to improve the device efficiency.

Typically, a DSSC comprises a dye-sensitized mesoporous-TiO_2-based photoanode, a redox couple electrolyte, and a platinum counter electrode. Photons with sufficient energy excite the dye molecules, followed by a rapid injection of electrons into the conduction band of TiO_2 nanoparticles, thereby oxidizing the dye molecule. The redox couple electrolyte subsequently reduces the dye molecule to its ground state while the electrolyte is regenerated at the counter electrode, resulting in open circuit voltage (V_{OC}) and short circuit current (J_{SC}). Recently, Daeneke et al. reported a DSSC study using ferrocenyl derivatives as redox electrolytes to understand the variation of dye regeneration efficiency with the change in ferrocene/ferrocenium redox potential.[11] This and a handful of other reports showed that ferrocenyl compounds are mostly used as redox couples and have never been used as effective sensitizers in DSSC due to their comparatively larger band gap that can only absorb a very small part of the solar spectrum.[11] Thus, designing a ferrocenyl derivative that can absorb a significant part of visible light that could not only act as a photon absorber but also, because of its intrinsic redox properties, would be able to regenerate the dye after the photogenerated electron has been transferred to the TiO_2 layer would obviate any additional redox electrolyte in the solar cell device. In that case, a ferrocenyl photon absorber can play the dual role of a dye and a redox system.

We have been, for some time, working on a variety of ferrocene-based molecular systems ranging from ferrocenylhydrazones to heterobimetallic ferrocenylchalcones, ferrocene-based cluster compounds, ferrocenyldithiocarboxylates, and multiferrocenyl entities and studied their electrochemical and photophysical properties.[12] While working on such systems, we came across a range of donor−acceptor type molecules which showed wide absorption in the visible region and discrete redox potential. Therefore, we focused our study on the exploration of some novel ferrocene-based donor−acceptor compounds as bifunctional molecules to work both as a dye and a redox electrolyte. Recently, a great deal of research has been focused on improving the performance of dye-sensitized solar cells (DSSC) by using various approaches such as structural modification of the dye and surface treatment of QDs which

Received: February 20, 2018

DOI: 10.1021/acs.organomet.8b00104

show a sharp increase in the absorptivity, sensitization properties, and power conversion efficiency.[13]

In this report, we describe a novel synthetic method to prepare donor−acceptor type ferrocenylcyanovinyl compounds using a superior solvent-free synthesis technique and study their photovoltaic characteristics by fabricating a DSSC device without using any additional redox electrolyte. We anticipated that the ferrocenyl-cyanovinyl-based donor−acceptor systems will absorb photons within a wide spectrum due to their donor−acceptor properties and in addition will also act as a ferrocenyl-based redox couple. Indeed, the electrolyte-free dye-sensitized solar cell gave an excellent open circuit voltage of 0.84 V, which is higher than the open circuit voltage achieved in a conventional ruthenium-based DSSC.[13c,g−k]

Use of solid inorganic supports for solvent-free organic reactions has attracted global attention due to their ability to perform reactions under mild conditions and easy product isolation methods.[14,15] Solid-state Knoevenagel condensation involving an organic substrate on an inorganic support such as Al_2O_3, SiO_2, KF/Al_2O_3, KOH/SiO_2, etc. have been well studied, while that involving organometallic moieties has not been explored extensively.[15,16] Therefore, to understand the wider scope of solid-supported reactions, we identified red mud (RM) as a possible support due to its metal oxide content and alkalinity and explored its potential in organometallic Knoevenagel reactions. Red mud (RM) is a toxic solid waste produced in the process of alumina extraction and gives rise to major environmental pollution. Thus, a solid-phase reaction of ferrocenylaldehyde and 1,1′-ferrocenyldicarboxyaldehyde with cyanoethylacetoacetate was investigated using red mud (RM) as a solid support. Equivalent amounts of the reactants were added to solid red mud powder, and the reaction mixture was thoroughly mixed and stirred at room temperature for 3 h. After the reaction, the mixture was extracted in ethyl acetate solvent and dried under vacuum. TLC showed the formation of a pink product which was purified by short-column chromatography for spectroscopic characterization and further study. Characterization using infrared, NMR, and mass spectroscopic techniques revealed the formation of 1-[{(η^5-C_5H_5)Fe(η^5-C_5H_4)CH=C(CN)CO_2Et}] (**1**) and 1,1′-[{Fe(η^5-C_5H_4)CH=C(CN)-CO_2Et}$_2$] (**2**) in high yields as shown in Scheme 1 (Text S1).

Scheme 1. Synthesis of Compounds 1, 2, 4 and 5

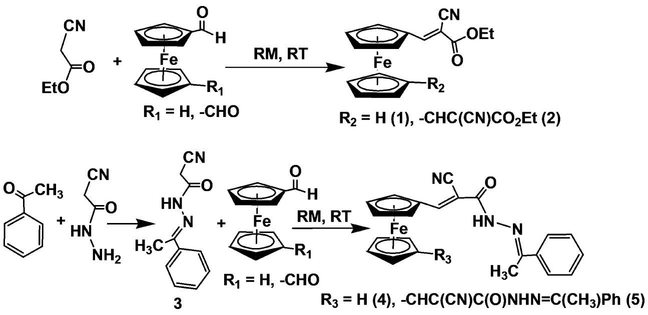

A single crystal, grown from a dichloromethane/*n*-hexane solvent mixture at −10 °C, was used for a single-crystal X-ray diffraction study. The molecular structure of **2** confirms the presence of a disubstituted ferrocenyl framework with a partially staggered conformation having a torsional angle of 50.84° between the two chains. Both of the chains containing a −CHC(CN)CO_2Et unit are attached to two different cyclopentadienyl rings of the ferrocene moiety (Figure S6). To understand the scope for the use of red mud in general reactions related to Knoevenagel condensation, a hydrazone-based derivative (**3**) containing a methylene active group was prepared using a modified solid-state procedure. Cyanoacetylhydrazone (**3**) was then reacted with ferrocenylmonoaldehyde using a solid-supported reaction process in the presence of red mud to obtain the two new ferrocene-based hydrazone compounds [{(η^5-C_5H_5)Fe(η^5-C_5H_4)CH=C(CN)C(O)NHN=C(CH_3)-Ph}] (**4**) and [{(η^5-C_5H_4)Fe(η^5-C_5H_4)}{CH=C(CN)C(O)-NHN=C(CH_3)Ph}$_2$] (**5**) (Scheme 1). Compounds **4** and **5** have been characterized by IR, NMR and mass spectroscopic techniques (Text S1).

The electrochemical properties of compounds **1**−**5** have been examined in acetonitrile solution using 0.1 M tetrabutylammonium perchlorate (TBAP) salt by cyclic voltammetry (CV) and differential pulse voltammetry (Figure S7). Compound **1**, involving a ferrocenyl moiety linked to one cyanovinyl group, exhibited a reversible redox process at +0.61 V vs SCE due to the Fe(II)/Fe(III) redox couple, while compound **2** with disubstituted cyanovinyl chains at the two cyclopentadienyl rings showed the redox process at much higher potential (+0.87 V vs SCE), making the molecule difficult to oxidize. However, when the cyanovinyl ester group in **1** was replaced with cyanovinylhydrazone in compound **4**, the redox process becomes slightly easier, showing the Fe(II)/Fe(III) couple at 0.57 V vs SCE. The same trend has been observed with compound **5**, which contains two cyanovinylhydrazone chains attached to the Cp rings; it shows an oxidation potential at $E_{1/2}$ = 0.76 V vs SCE. Incorporation of the ferrocenyl substituent within the cyanovinyl ester fragment significantly influences the donor−acceptor and absorption properties of **1** and **2**. The solution-based UV−visible absorption spectra of **1** and **2** exhibit major bands in the 320, 335, 380, 425, 510, and 521 nm regions (Figure S13). The thin film absorption spectra were obtained by depositing the compound on a mesoporous-TiO_2-coated glass substrate by dip-coating. The absorption spectra for both compounds reveal wide absorption in the visible region in the 400−700 nm region, as shown in Figure S14. The onset absorption edges of **1** and **2** are 703 and 679 nm, respectively, corresponding to optical band gaps of 1.8 eV.

The absorption spectra of **1** and **2** were correlated by TD-DFT calculations and are consistent with the experimental data (Figure S9). A corresponding energy level diagram has been constituted with the help of redox potential data and thin film absorption spectra, as given in Figure 1a.

The wide absorption properties in the visible region and the measured diode characteristics (Figure S10) prompted us to evaluate the DSSC performance of compounds **1** and **2** as bifunctional molecules to work as both a dye and a redox couple system. TiO_2/[**1**]- and TiO_2/[**2**]-based mesoporous heterojunctions were used to study the electrolyte-free sensitized solar cells. A schematic representation of the TiO_2/[**1**]/Pt mesoporous heterojunction is shown in Figure S15. A complete pore filling of the mesoporous TiO_2 was achieved by dipping the meso-TiO_2-coated FTO into a 10 mM solution of **1**, as shown in cross-sectional FESEM images (Figure S11). Nonlinear diode like characteristics of TiO_2/[**1**],[**2**]/Pt in the current density vs voltage (*J*−*V*) curve under dark conditions confirms the formation of a heterojunction at the meso-TiO_2/[**1**] and meso-TiO_2/[**2**] interfaces (Figure S10). Photovoltaic performances of these mesoporous heterojunction solar cells were measured in air at 1 sun illumination (100 mW/cm^2), and

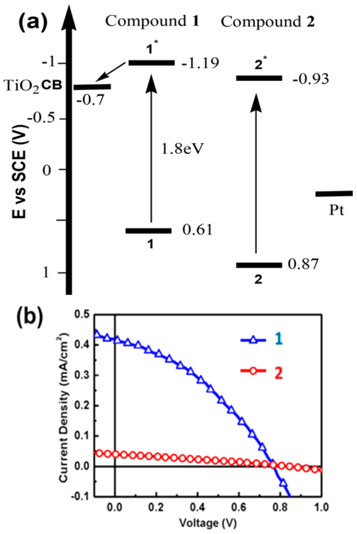

Figure 1. (a) Energy level diagram, (b) *J-V* characteristics of the heterojunction solar cells under light using **1** and **2** as the absorbers.

typical *J*−*V* characteristics are plotted in Figure 1b and their characteristic parameters are given in Table 1. Under 1 sun illumination, a short-circuit photocurrent density (J_{SC}) of 0.41 mA/cm^2, open-circuit voltage (V_{OC}) of 763 mV, and fill factor (FF) of 35% were observed for **1**-based devices. A higher V_{OC} value of 841 mV was observed, and a short-circuit photocurrent density, J_{SC}, of 39 μA/cm^2 was achieved for the device fabricated using compound **2**. The study shows that a higher V_{OC} has been obtained with an electrolyte-free DSSC device in comparison to the reported performance using I_2/I^- as redox electrolyte.[13j,17]

Table 1. Photovoltaic Parameters Derived from the *J*−*V* Characteristics of the Device

compound	J_{SC} (mA/cm^2)	V_{OC} (mV)	FF (%)	η (%)
1	0.41	763	35	0.10
2	0.039	841	28	9.18×10^{-3}

In order to ascertain the nature of the orbitals involved during DSSC performances, DFT calculations using a LANL2DZ basis set at the B3LYP level were performed on the optimized structures of the compound and their oxidized species. DFT calculations were carried out for compounds **1** and **2** in the gas phase and were fully optimized without any constraint. The calculation reveals that the HOMO for both compounds **1** and **2** is mainly localized on the ferrocenyl fragment, while the LUMO is largely distributed on the cyanoethyl acetate chain (Tables S2 and S5). A natural electron population analysis (NPA) was also performed on **1** and **2** as well as on their respective 1e$^-$-oxidized species. The natural electron spin populations ($\alpha-\beta$) at the iron atom in $\mathbf{1}^+$ and $\mathbf{2}^+$ species are 1.25494 and 1.29594, respectively, which indicate that during oxidation the electron is released mainly from the ferrocenyl iron center. The gross natural electron spin populations of the cyanovinyl ester fragment in the oxidized species of **1** and **2** are 0.631 au and 0.514, 0.628 au, respectively, which reveal significant charge delocalization within the cyanovinyl fragment on oxidation. The calculations also reveal two different spin densities for the two cyanovinyl ester chains in compound **2**, suggesting unsymmetrical α,β spins between the two cyanovinyl chains (Table S1). To correlate the experimentally observed V_{OC} data for the DSSC, fabricated using **1** and **2** in an electrolyte-free system, we conducted DFT calculations on neutral and oxidized species. The calculation reveals an electron transfer mechanism involving a ground state (**1**, **2**) which on photoexcitation goes to states **1***, **2*** and subsequently injects electrons to the TIO_2 CB, oxidizing the molecule to $\mathbf{1}^+$, $\mathbf{2}^+$. The calculated MOs of the optimized $\mathbf{1}^+$, $\mathbf{2}^+$ are energetically more stable than the platinum work function and become reduced by the Pt cathode to regenerate the dye (**1**, **2**). Figure S16 shows a tentative schematic representation of the electron transfer. It has been understood that the presence of an optimized oxidized state restricts the recombination process and also helps in easier reduction of the dye using the Pt cathode. The proposed electron transfer process also reveals that the role of the redox couple for the regeneration of dye in the usual DSSC has been served here by the dye itself due to the presence of an intrinsic ferrocenyl system. Therefore, the bifunctionality of molecules **1** and **2**, to serve as redox electrolytes in addition to absorber dyes, make the systems potential candidates for harvesting solar energy. In summary, a novel synthetic method with a high yield of the product has been introduced to prepare some ferrocene-based donor−acceptor molecules that can absorb in visible light within a wide energy range. The presence of both a ferrocene moiety and a cyanovinyl chain with wide absorption properties prompted us to fabricate a unique solar cell device without any additional redox couple. The electrolyte-free dye-sensitized solar cell gave an unprecedented open circuit voltage of 0.76 V for **1** and 0.84 V for **2**. Our current effort has been focused on the fabrication of an electrolyte-free solar cell device using long-chain donor−acceptor ferrocenyl derivatives to increase the efficiency of the photovoltaic cell.

■ ASSOCIATED CONTENT

Ⓢ Supporting Information

The Supporting Information is available free of charge on the ACS Publications website at DOI: 10.1021/acs.organomet.8b00104.

> Characterization data, crystallographic data, calculation details, and experimental section (PDF)

Accession Codes

CCDC 1563814 contains the supplementary crystallographic data for this paper. These data can be obtained free of charge via www.ccdc.cam.ac.uk/data_request/cif, or by emailing data_request@ccdc.cam.ac.uk, or by contacting The Cambridge Crystallographic Data Centre, 12 Union Road, Cambridge CB2 1EZ, UK; fax: +44 1223 336033.

■ AUTHOR INFORMATION

Corresponding Authors

*S.C.: tel, +91 661 2462656; fax, +91 661 2472926; e-mail, saurav@nitrkl.ac.in.
*A.B.: e-mail, ashok.bera@iitjammu.ac.in.

ORCID

S. M. Mobin: 0000-0003-1940-3822
S. Chatterjee: 0000-0002-6290-4342

Notes

The authors declare no competing financial interest.

■ ACKNOWLEDGMENTS

S.C. is grateful to the Department of Science and Technology (SERB), Government of India, for research funding (No. SB/

S1/IC-30/2013). A.B. is thankful to DST-INSPIRE for financial support.

■ REFERENCES

(1) (a) Vanicek, S.; Podewitz, M.; Stubbe, J.; Schulze, D.; Kopacka, H.; Wurst, K.; Meller, T.; Lippmann, P.; Haslinger, S.; Schottenberger, H.; Liedl, K. R.; Ott, I.; Sarkar, B.; Bildstein, B. *Chem. - Eur. J.* **2018**, *24*, 3742−3753. (b) Teator, A. J.; Lastovickova, D. N.; Bielawski, C. W. *Chem. Rev.* **2016**, *116*, 1969−1992. (c) Neumann, P.; Dib, H.; Caminade, A. M.; Hey-Hawkins, E. *Angew. Chem., Int. Ed.* **2015**, *54*, 311−314. (d) Teimuri-Mofrad, R.; Rahimpour, K.; Ghadari, R. *J. Organomet. Chem.* **2017**, *846*, 397−406. (e) De Silva, A. P. *Nature* **2007**, *445*, 718−719. (f) Cook, T. R.; Dogutan, D. K.; Reece, S. Y.; Surendranath, Y.; Teets, T. S.; Nocera, D. G. *Chem. Rev.* **2010**, *110*, 6474−6502. (g) Alizadeh, T.; Akhoundian, M.; Ganjali, M. R. *New J. Chem.* **2018**, *42*, 4719−4727.

(2) (a) Lu, J.; Chamberlin, D.; Rider, D. A.; Liu, M.; Manners, I. *Nanotechnology* **2006**, *17*, 5792−5797. (b) Ren, T. *Organometallics* **2005**, *24*, 4854−4870.

(3) Ornelas, C.; Aranzaes, J. R.; Cloutet, E.; Alves, S.; Astruc, D. *Angew. Chem., Int. Ed.* **2007**, *46*, 872−877.

(4) (a) Lyons, D. M.; Mohanraj, J.; Accorsi, G.; Armaroli, N.; Boyd, P. D. W. *New J. Chem.* **2011**, *35*, 632−639. (b) Xiang, J.; Pi, X.; Chen, X.; Xiang, L.; Yang, M.; Ren, H.; Shen, X.; Qi, N.; Deng, C. *Biosens. Bioelectron.* **2017**, *96*, 268−274. (c) Zou, W.; Pang, W.; Chen, C. *Inorg. Chem. Front.* **2017**, *4*, 795−800.

(5) (a) Hildebrandt, A.; Lang, H. *Organometallics* **2013**, *32*, 5640−5656. (b) Ren, T. *Chem. Rev.* **2008**, *108*, 4185−4207. (c) Bruce, M. I.; Low, P. J. *Adv. Organomet. Chem.* **2004**, *50*, 179−444. (d) Szafert, S.; Gladysz, J. A. *Chem. Rev.* **2006**, *106*, PR1−PR33; **2003**, *103*, 1−33.

(6) (a) Sakamoto, R.; Murata, M.; Nishihara, H. *Angew. Chem., Int. Ed.* **2006**, *45*, 4793−4795. (b) Engtrakul, C.; Sita, L. R. *Nano Lett.* **2001**, *1*, 541−549. (c) Wagner, M. *Angew. Chem., Int. Ed.* **2006**, *45*, 5916−5918. (d) Dong, T. Y.; Chang, L. S.; Tseng, I. M.; Huang, S. J. *Langmuir* **2004**, *20*, 4471−4479. (e) Skibar, W.; Kopacka, H.; Wurst, K.; Salzmann, C.; Ongania, K.-H; Biani, F. F.; Zanello, P.; Bildstein, B. *Organometallics* **2004**, *23*, 1024−1041. (f) Getty, S. A.; Engtrakul, C.; Wang, L.; Liu, R.; Ke, S.-H; Baranger, H. U.; Yang, W.; Fuhrer, M. S. L; Sita, R. *Phys. Rev. B: Condens. Matter Mater. Phys.* **2005**, *71*, 241401.

(7) (a) Shoji, T.; Ito, S.; Okujima, T.; Morita, N. *Eur. J. Org. Chem.* **2011**, *2011*, 5134−5140. (b) Mata, J.; Uriel, S.; Peris, E.; Llusar, R.; Houbrechts, S.; Persoons, A. *J. Organomet. Chem.* **1998**, *562*, 197−202. (c) Jordan, M.; Kivala, M.; Boudon, C.; Gisselbrecht, J. P.; Schweize, W. B.; Seiler, P.; Diederich, F. *Chem. - Asian J.* **2011**, *6*, 396−401.

(8) (a) Green, M. L.; Marder, S. R.; Thompson, M. E.; Bandy, J. A.; Bloor, D.; Kolinsky, P. V.; Jones, R. J. *Nature* **1987**, *330*, 360−362. (b) Coe, B. J.; Jones, C. J.; McCleverty, J. A.; Cross, G. *J. Organomet. Chem.* **1994**, *464*, 225−232. (c) Kato, S.; Kivala, M.; Schweizer, W. B.; Boudon, C.; Gisselbrecht, J. P.; Diederich, F. *Chem. - Eur. J.* **2009**, *15*, 8687−8691.

(9) (a) Thomas, K. R. J; Lin, J. T.; Wen, Y. S. *J. Organomet. Chem.* **1999**, *575*, 301−309. (b) Pal, S. K.; Krishnan, A.; Das, P. K.; Samuelson, A. S. *J. Organomet. Chem.* **2000**, *604*, 248−259. (c) Yin, X.; Li, Y.; Zhu, Y.; Jing, X.; Li, Y.; Zhu, D. *Dalton Trans.* **2010**, *39*, 9929−9935.

(10) (a) Blanchard-Desce, M.; Runser, C.; Fort, A.; Barzoukas, M.; Lehn, J. M.; Bloy, V.; Alain, V. *Chem. Phys.* **1995**, *199*, 253−261. (b) Moore, J. A.; Chesney, A.; Bryce, R. M.; Batsanov, S. A.; Perepichka, F. I.; Khodorkovsky, V. *Eur. J. Org. Chem.* **2001**, *2001*, 2671−2687.

(11) (a) Daeneke, T.; Mozer, A. J.; Uemura, Y.; Makuta, S.; Fekete, M.; Tachibana, Y.; Koumura, N.; Bach, U.; Spiccia, L. *J. Am. Chem. Soc.* **2012**, *134*, 16925−16928. (b) Daeneke, T.; Mozer, A. J.; Kwon, T.-H; Duffy, N. W.; Holmes, A. B.; Bach, U.; Spiccia, L. *Energy Environ. Sci.* **2012**, *5*, 7090−7099. (c) Chauhan, R.; Trivedi, M.; Bahadur, L.; Kumar, A. *Chem. - Asian J.* **2011**, *6*, 1525−1532. (d) An, M.; Kim, S.; Hong, J.-D. *Bull. Korean Chem. Soc.* **2010**, *31*, 3272−3278.

(12) (a) Mishra, S.; Dewangan, S.; Giri, S.; Mobin, S. M.; Chatterjee, S. *Eur. J. Inorg. Chem.* **2016**, *2016*, 5485−5496. (b) Tirkey, V.; Mishra, S.; Dash, H. R.; Das, S.; Nayak, B. P.; Mobin, S. M.; Chatterjee, S. *J. Organomet. Chem.* **2013**, *732*, 122−129. (c) Patel, S. K.; Tirkey, V.; Mishra, S.; Dash, H. R.; Das, S.; Shukla, M.; Saha, S.; Mobin, S. M.; Chatterjee, S. *J. Organomet. Chem.* **2014**, *749*, 75−82. (d) Mishra, S.; Tirkey, V.; Ghosh, A.; Dash, H. R.; Das, S.; Shukla, M.; Saha, S.; Mobin, S. M.; Chatterjee, S. *J. Mol. Struct.* **2015**, *1085*, 162−172. (e) Tirkey, V.; Boddhula, R.; Mishra, S.; Mobin, S. M.; Chatterjee, S. *J. Organomet. Chem.* **2015**, *794*, 88−95. (f) Mathur, P.; Chatterjee, S.; Avasare, V. D. *Adv. Organomet. Chem.* **2007**, *55*, 201−277.

(13) (a) Choi, H.; Chen, Y.-S.; Stamplecoskie, K. G.; Kamat, P. V. *J. Phys. Chem. Lett.* **2015**, *6*, 217−223. (b) Choi, H.; Kamat, P. V. *J. Phys. Chem. Lett.* **2013**, *4*, 3983−3991. (c) Chen, C.-Y.; Wang, M.; Li, J.-Y.; Pootrakulchote, N.; Alibabaei, L.; Ngoc-le, C.-H.; Decoppet, J.-D.; Tsai, J.-H.; Gratzel, C.; Wu, C.-G.; et al. *ACS Nano* **2009**, *3*, 3103−3109. (d) Litke, S. V.; Ershov, A. Y.; Meyer, T. J. *J. Phys. Chem. A* **2014**, *118*, 6216−6222. (e) Kamat, P. V. *J. Phys. Chem. Lett.* **2013**, *4*, 908−918. (f) Lan, X.; Masala, S.; Sargent, E. H. *Nat. Mater.* **2014**, *13*, 233−240. (g) Jiang, K.-J.; Masaki, N.; Xia, J.-B.; Noda, S.; Yanagida, S. *Chem. Commun.* **2006**, 2460−2462. (h) Kuang, D.; Ito, S.; Wenger, B.; Klein, C.; Moser, J.-E.; Humphry-Baker, R.; Zakeeruddin, S. M.; Gratzel, M. *J. Am. Chem. Soc.* **2006**, *128*, 4146−4154. (i) Hagfeldt, A.; Gratzel, M. *Acc. Chem. Res.* **2000**, *33*, 269−277. (j) Onozawa-Komatsuzaki, N.; Yanagida, M.; Funaki, T.; Kasuga, K.; Kazuhiro, S.; Sugihara, H. *Sol. Energy Mater. Sol. Cells* **2011**, *95*, 310−314. (k) Onozawa-Komatsuzaki, N.; Yanagida, M.; Funaki, T.; Kasuga, K.; Sayama, K.; Sugihara, H. *Inorg. Chem. Commun.* **2009**, *12*, 1212−1215.

(14) (a) Toda, F. *Acc. Chem. Res.* **1995**, *28*, 480−486. (b) Cave, G. W. V; Raston, C. L.; Scott, J. L. *Chem. Commun.* **2001**, 2159−2169. (c) Grant, J. T.; Venegas, J. M.; McDermott, W. P.; Hermans, I. *Chem. Rev.* **2018**, *118*, 2769. (d) Tanaka, K.; Toda, F. *Solvent-free Organic Synthesis*; Wiley-VCH: Weinheim, Germany, 2003. (e) Hernández, J. G.; Juaristi, E. *J. Org. Chem.* **2010**, *75*, 7107−7111. (f) Singh, M. S.; Chowdhury, S. *RSC Adv.* **2012**, *2*, 4547−4592. (g) Rahman, A.; Jonnalagadda, S. B. *Catal. Lett.* **2008**, *123*, 264−268. (h) Laszlo, P.; Pennetreau, P. *Tetrahedron Lett.* **1985**, *26*, 2645−2648. (i) Kloetstra, K. R.; Bekkum, H. V. *J. Chem. Soc., Chem. Commun.* **1995**, 1005−1006. (j) Choudary, B. M.; Kantam, M. L.; Rahman, A.; Reddy, Ch. V. R. *J. Mol. Catal. A: Chem.* **2003**, *206*, 145−151. (k) Wada, S.; Suzuki, H. *Tetrahedron Lett.* **2003**, *44*, 399−401. (l) *Catalysts for fine chemicals synthesis, Microporous and Mesoporous Solid Catalysts*; Roberts, S. M., Ed.; Wiley-VCH: New York, 2006; Vol. 4.

(15) (a) Pullabhotla, V. S. R. R; Rahman, A.; Jonnalagadda, S. B. *Catal. Commun.* **2009**, *10*, 365−369. (b) Texier-Boullet, F.; Foucaud, A. *Tetrahedron Lett.* **1982**, *23*, 4927−4928. (c) Hellwinkel, D.; Göke, K. *Synthesis* **1995**, *1995*, 1135−1141. (d) Detty, M. R.; Eachus, R. S.; Simicropi, J. A.; Lenhard, J. R.; McMillan, M.; Lauzafame, A. M.; Luss, H. R.; Young, R.; Eilers, J. E. *J. Org. Chem.* **1995**, *60*, 1674−1685.

(16) (a) Stanković, E.; Toma, S.; Boxel, R. V.; Asselberghs, I.; Persoons, A. *J. Organomet. Chem.* **2001**, *637-639*, 426−434. (b) Cooke, G.; Palmer, H. M.; Schulz, O. *Synthesis* **1995**, *1995*, 1415−1418. (c) Cooke, G.; Schulz, O. *Synth. Commun.* **1996**, *26*, 2549−2560. (d) Villemin, D.; BenAlloum, A. *Phosphorus, Sulfur Silicon Relat. Elem.* **1993**, *79*, 33−41. (e) Stanković, E.; Elekčo, P.; Toma, S. *Chem. Pap.* **1996**, *50*, 68−71.

(17) (a) Krishna, N. V.; Krishna, J. V. S; Singh, S. P.; Giribabu, L.; Han, L.; Bedja, I.; Gupta, R. K.; Islam, A. *J. Phys. Chem. C* **2017**, *121*, 6464−6477. (b) Polo, A. S.; Itokazu, M. K.; Iha, N. Y. M. *Coord. Chem. Rev.* **2004**, *248*, 1343−1361. (c) Nazeeruddin, M. K.; Pèchy, P.; Renouard, T.; Zakeeruddin, S. M.; Humphry-Baker, R.; Comte, P.; Liska, P.; Cevey, L.; Costa, E.; Shklover, V.; Spiccia, L.; Deacon, G. B.; Bignozzi, C. A.; Grätzel, M. *J. Am. Chem. Soc.* **2001**, *123*, 1613−1624.

DOI: 10.1021/acs.organomet.8b00104